

# Stagnation-Point Pressure Distribution and Wall Shear Stress: Numerical Simulation and Similarity Solution

Vai Kuong Sin and Tai Yin Tong

**Abstract**—Two-dimensional stagnation-point flow in three different aspect ratios is studied by solving the full Navier-Stokes equations with the computational fluid dynamics (CFD) software of STAR-CD and results are compared with those obtained from the similarity solution. Pressure variation in the directions normal and parallel to the wall, as well as wall shear stress along the wall are investigated. Results show that pressure profiles are in good agreement for both numerical simulation and similarity solution at high aspect ratio in the stagnation-point region. Discrepancy of results in pressure profiles increases as aspect ratio decreases and in region which is away from the stagnation-point flow. It is found that wall shear stress is proportional to the distance from the stagnation-point along the wall as expected by similarity solution.

**Index Terms**— Computational Fluid Dynamics, Similarity Solution, Stagnation-Point Flow.

## I. INTRODUCTION

Consider a fluid stream whose velocity vector coinciding with the  $y$  axis as shown in Figure 1. The fluid impinges on a plane boundary which coincides with the  $x$  axis. Stagnation-point flow has been found in numerous applications in engineering and technology [1]. It can be located in the stagnation region of flow passing any shape of body, i.e., pier and aerofoil. Hiemenz [2] discovered that stagnation-point flow can be analyzed by the Navier-Stokes (NS) equations through similarity solution in which the number of variables can be reduced by one or more by a coordinate transformation. Similarity solution is limited to certain types of flow with certain boundary conditions and the result is valid in specific region of the flow. On the other hand, numerical simulation of the NS equations in stagnation-point flow can give a result which can be interpreted from different point of view. In previous study [3][4] of velocity distribution and boundary layer thickness in 2-D stagnation-point flow, it is found that boundary layer thickness obtained in numerical calculation is not constant along the wall, but decreases slightly along the wall. The difference of the boundary layer thickness obtained from

numerical simulation and similarity solution is small for low aspect ratio and close to the stagnation point. The paper is to use computational fluid dynamics software to solve the Navier-Stokes equations for pressure in two-dimensional stagnation-point flow and the results are compared with those obtained from similarity solution.

## II. GOVERNING EQUATIONS

The 2-dimensional Navier-Stokes equations for stagnation-point flow shown in Figure 1 can be written as [5]

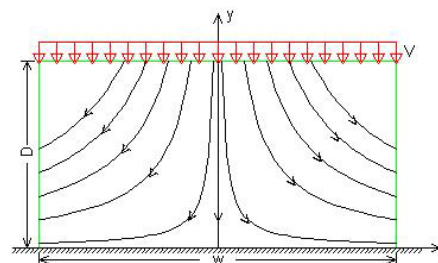


Fig. 1 Configuration of stagnation-point flow

$$\nabla \cdot \vec{V} = 0 \quad (1)$$

$$(\vec{V} \cdot \nabla)u = -\frac{1}{\rho} \frac{\partial p}{\partial x} + \nu \Delta u \quad (2)$$

$$(\vec{V} \cdot \nabla)v = -\frac{1}{\rho} \frac{\partial p}{\partial y} + \nu \Delta v \quad (3)$$

Where  $\vec{V} = u\mathbf{i} + v\mathbf{j}$  is velocity with components  $u$  and  $v$  along the  $x$  and  $y$  axis,  $p$  is pressure,  $\nu$  is kinematic viscosity of fluid, and  $\Delta$  is the two-dimensional Laplace operator. The boundary conditions are  $u=v=0$  at  $y=0$  and  $u=0, v=-V$  when  $y \rightarrow \infty$ .

### A. Similarity Solution

For 2-D planar incompressible flow, (1) can be satisfied automatically by introducing a combined stream function  $\psi(x, y)$ :

$$u = \frac{\partial \psi}{\partial y} \quad \text{and} \quad v = -\frac{\partial \psi}{\partial x}$$

For stagnation flow without friction (ideal fluid flow), the stream function  $\psi \propto xy$  or may be written as

Manuscript received March 23, 2009. This work is partially supported by University of Macau under grants RG072/07-08S/SVK/FST, RG060/08-09S/SVK/FST, and UL020/08-Y2/MAT/JXQ01/FST to V. K. Sin.

V. K. Sin is with the Department of Electromechanical Engineering, University of Macau, Macao SAR, China (corresponding author to provide phone: 853-83974357; fax: 853-28838314; e-mail: vksin@umac.mo).

T. Y. Tong is graduate student in the Department of Electromechanical Engineering, University of Macau, Macao SAR, China (e-mail: ma76512@umac.mo).

$$\psi = \psi_1 = Bxy \quad (4)$$

Where  $B$  is a constant and from which

$$u_1 = Bx \quad \text{and} \quad v_1 = -By. \quad (5)$$

We have  $u_1=0$  at  $x=0$  and  $v_1=0$  at  $y=0$ . The point  $x=0$  and  $y=0$  is a stagnation point. However, the no-slip boundary at wall ( $y=0$ ) cannot be satisfied.

For (real) viscous fluid,  $\psi_1$  can be modified as

$$\psi = Bxf(y). \quad (6)$$

In this way, the no-slip boundary condition can be satisfied at  $y=0$ . Note that the  $x$ -dependence relationship,  $\psi \propto x$ , is still the same as that for  $\psi_1$  in (4). The velocity components corresponding to (5) are

$$u = Bxf'(y) \quad \text{and} \quad v = -Bf(y) \quad (7)$$

Where  $f' = df/dy$ . Substituting (7) into (3), we have

$$-\frac{1}{\rho} \frac{\partial p}{\partial y} = B^2 ff'' + \nu Bf''',$$

which is function of  $y$  only and gives

$$\frac{\partial^2 p}{\partial x \partial y} = 0. \quad (8)$$

With (8), pressure can be eliminated by differentiating (2). The result is

$$f^{iv} + \frac{B}{\nu} (ff'')' - \frac{B}{\nu} (f'^2)' = 0. \quad (9)$$

The no-slip condition at  $y=0$  implies that

$$f'(0) = f(0) = 0.$$

For region sufficiently away from the wall, the viscous effect is negligible and the flow is expected to match with the inviscid flow result. Thus we require

$$f'(\infty) = 1 \quad \text{and} \quad f(\infty) = y \quad (10)$$

by comparing (7) with (5). Integrating (9), we have

$$f''' + \frac{B}{\nu} ff'' - \frac{B}{\nu} f'^2 = C. \quad (11)$$

The constant  $C$  can be determined from (10) and is

$$C = -\frac{B}{\nu}.$$

Note that the conditions,  $f''(\infty) = f'''(\infty) = 0$ , have been used to ensure that the flow matches smoothly with the inviscid flow at  $y \rightarrow \infty$ . Thus (11) becomes

$$f'''' + \frac{B}{\nu} ff'' + \frac{B}{\nu} (1 - f'^2) = 0. \quad (12)$$

Note that  $B$  has the dimension as “1/time” and  $f$  has dimension as “length”. By introducing the dimensionless variables

$$\eta = y\sqrt{B/\nu} \quad \text{and} \quad F(\eta) = \sqrt{B/\nu} f(y), \quad (13)$$

such that

$$u = BxF'(\eta) \quad \text{and} \quad v = -\sqrt{B\nu}F(\eta),$$

(12) becomes

$$F'''' + FF'' + (1 - F'^2) = 0, \quad (14)$$

which is in dimensionless form, and is solved subject to the following boundary conditions:

$$F(0) = F'(0) = F'(\infty) - 1 = 0. \quad (15)$$

Similarity solution [5] shows that region of nonzero vorticity, also known as boundary-layer thickness  $\delta_{99}$ , which is defined as the value of  $y$  such that  $u=0.99Bx$ , is constant along the boundary wall and is given by  $\delta_{99}=2.4(\nu/B)^{1/2}$ . It is noted that for 2-D plane stagnation-point flow as shown in Fig.1, the constant  $B$  is equal to  $V/D$  and  $\nu$  is kinematic viscosity of fluid which is chosen as water at 25°C and has the value of  $8.908728389 \times 10^{-7} \text{ m}^2/\text{s}$ . The two-point boundary value problem of (14) and (15) is solved numerically with Matlab build-in function `bvp4c.m` as illustrated in [6]

Once  $u$  and  $v$  are available, pressure in the flow can be obtained by integrating (2). The result is

$$\frac{p(x,\eta) - p_0}{\rho} = -\frac{1}{2} B^2 x^2 - \frac{1}{2} B \nu F^2 - B \nu F'. \quad (16)$$

Where  $p_0$  is the stagnation pressure at  $x=0, y=0$  and is setting to be zero in present study. Thus the pressure gradients in the direction parallel and normal to the wall are given by:

$$\frac{\partial p}{\partial x} = -\rho B^2 x \quad (17)$$

$$\frac{\partial p}{\partial y} = -\rho B \sqrt{B\nu} (FF' + F''') = O(\sqrt{\nu}). \quad (18)$$

Hence the pressure gradient in the direction normal to the wall is small with the order of magnitude of  $\sqrt{\nu}$  and is negligible for small fluid viscosity. Finally shear stress at the wall is defined as

$$\tau_w = \mu \left( \frac{\partial u}{\partial y} + \frac{\partial v}{\partial x} \right)_{y=0},$$

which can be expressed as

$$\tau_w = \mu B x F'''(0) \sqrt{\frac{B}{\nu}}. \quad (19)$$

### B. Numerical Simulation

As indicated in [7], a proof of uniqueness of a similarity solution of the stagnation-point flow is not available. Numerical solution is sought to solve stagnation-point flow problem by a commercial CFD software STAR-CD. STAR-CD employs implicit methods to solve the algebraic finite-volume equations resulting from the discretisation of the Navier-Stokes equations. Three implicit algorithms are available in STAR-CD. They are SIMPLE[8], PISO[9], and SIMPISO[10]. It is PISO method that is employed in this simulation. The acronym PISO stands for Pressure Implicit with Splitting of Operators. The PISO algorithm is a pressure-velocity calculation procedure developed originally for the non-iterative computation of unsteady compressible flows. It has been adapted successfully for the iterative solution of steady state problems. As a result of the decoupling of the equations for each dependent variable and subsequent linearization, large sets of linear algebraic equations are obtained and algebraic multigrid (AMG) method is chosen to solve matrix equations in STAR-CD. Boundary conditions are  $u=v=0$  at  $y=0$  and  $u=0, v=-V$  when  $y=D$ . Three cases with different aspect ratios (D/W) have been investigated in present stagnation-point flow study and detailed information is given in Table I. Rectangular finite volumes with non-uniform distribution is used to handle the large velocity gradient near the wall. Reynolds number, which is defined as  $Re=VD/\nu$ , is also given in Table I. Number of finite volumes being used in cases I, II, and III are 60,000, 80,000, and 200,000 respectively. The order of residuals is  $10^{-5}$  for all simulations.

|          | W (mm) | D(mm) | V(mm/s) | Re   |
|----------|--------|-------|---------|------|
| Case I   | 20     | 30    | 10      | 337  |
| Case II  | 20     | 40    | 10      | 449  |
| Case III | 20     | 100   | 10      | 1122 |

### III. NUMERICAL RESULTS AND COMPARISONS

Fig. 2 shows the pressure variation normal to the solid wall at  $x=0.001m, 0.0025m, \text{ and } 0.0075m$  for case I with low aspect ratio of  $D/W=1.5$ . Lines without markers denote results obtained from numerical simulation (NS) and lines with markers are from similarity solution (SS). Results obtained from those two methods are in good agreement in the region near the stagnation point and within the boundary layer, i.e.,  $x \leq 0.0025m, y \leq \delta_{SS} = 0.00392m$ . The difference increases as either  $x$  or  $y$  increases, i.e., away from the stagnation point. It is noted that pressure curves at  $x=0.001m$  and  $0.0025m$ , are close to each other for either similarity solution or numerical simulation. A large difference is observed at  $x=0.0075m$  from both methods. Also shown in Fig. 2 is the boundary layer thickness ( $\delta_{SS}$ ) obtained from similarity solution. As we increase the aspect ratio from  $D/W=1.5$  to  $D/W=2$  as shown in Fig. 3, the discrepancy of results from these two methods has been improved by about 50%. This can be seen even more clearly when we further increase the aspect ratio to  $D/W=5$  as shown in Fig. 4. In Fig. 4, all pressure curves almost fall on a single curve within the boundary layer. The difference of results is only observed in the region where it is out of the boundary layer and that difference is still much smaller than those obtained from low aspect ratio. It should be noted that in all three cases, the pressure gradient normal to the wall within the boundary layer thickness in small which is consistent with (18).

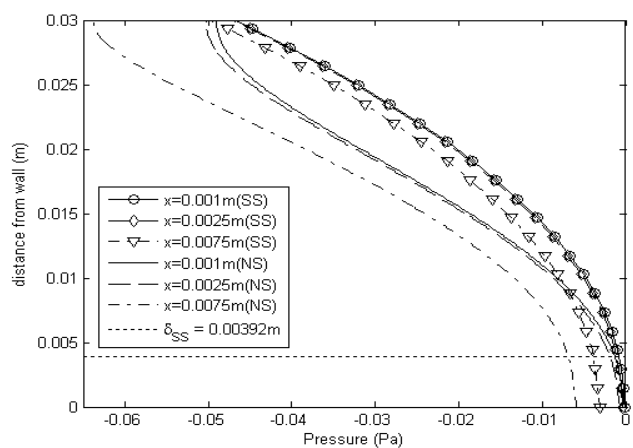


Fig. 2 Pressure profiles and boundary layer thickness of stagnation-point flow for case I

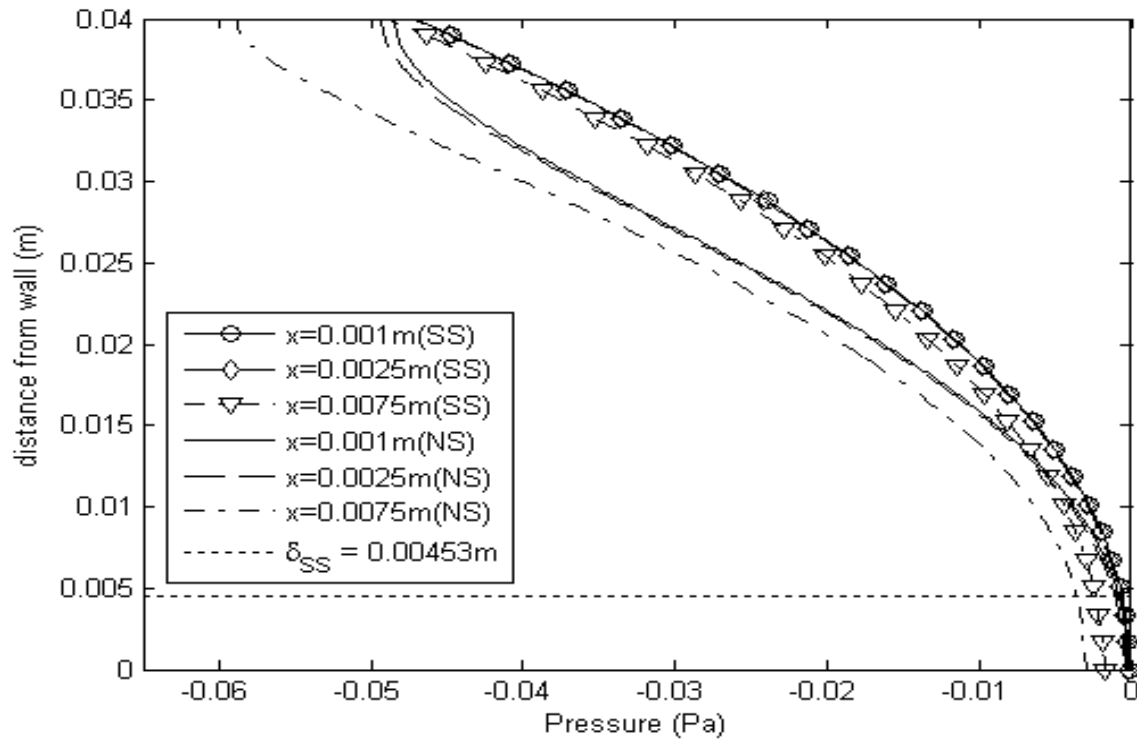


Fig. 3 Pressure profiles and boundary layer thickness of stagnation-point flow for case II

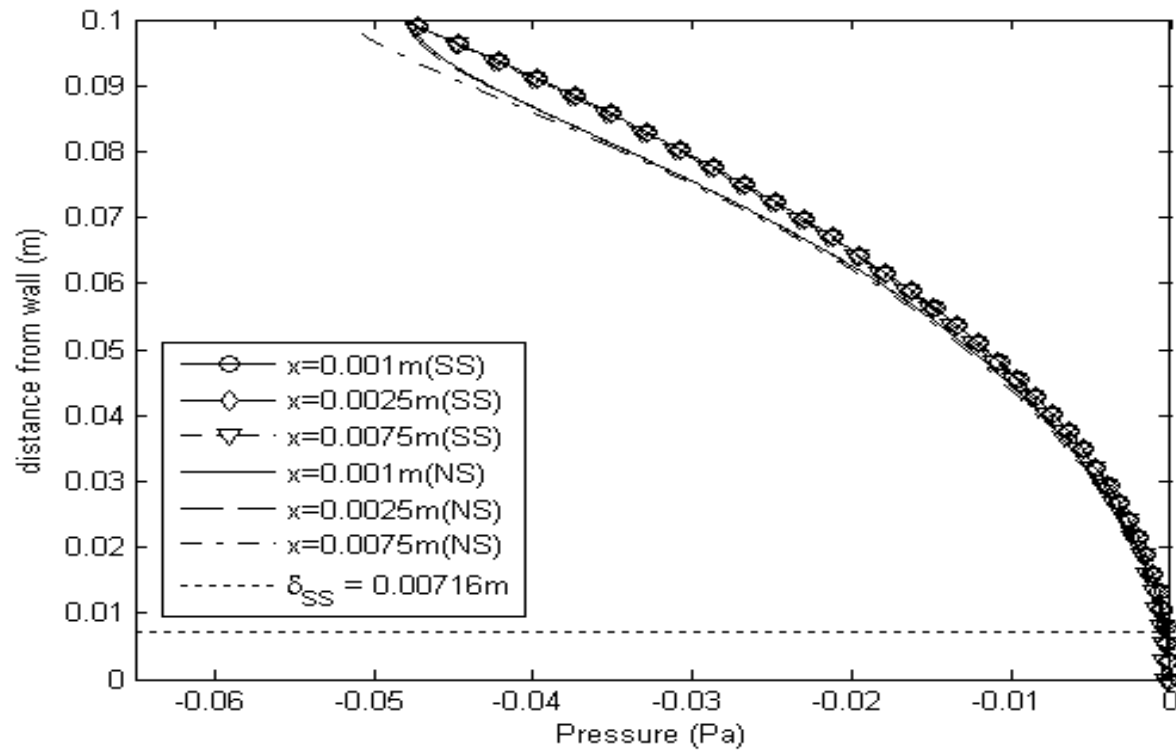


Fig. 4 Pressure profiles and boundary layer thickness of stagnation-point flow for case III

Pressure variations parallel to the wall within the boundary layer and outside the boundary layer are given in Figs. 5 and 6, respectively. Again lines without markers represent results obtained from numerical simulation (NS) while lines with markers are from similarity solution (SS). Fig. 5 shows that, within the boundary layer, i.e.,  $y=0.001\text{m}$ , the pressure variations parallel to the wall obtained by numerical simulation and similarity solution are very close for high aspect ratio. For low aspect ratio, they are still close near the stagnation point ( $x \leq 0.00025\text{m}$ ), but differ from each other when  $x$  is increasing. Nevertheless, the fact that pressure is proportional to  $x^2$  can be observed for all cases. Fig. 6 presents pressure variations parallel to the wall outside the

boundary layer at  $y=0.01\text{m}$ . Results obtained from both methods are in good agreement only for high aspect ratio. Discrepancy of results is observed even in the region of stagnation point for low aspect ratio. It should be noted that the trends of pressure profiles are similar to each other for all cases.

Distribution of wall shear stress is given in Fig. 7. All cases show that the wall shear stress is proportional to  $x$  except in the region close to the exit on both sides. This in fact is consistent with those indicated in (19). It is also found that wall shear stress by numerical simulation is always larger than those predicted by similarity solution.

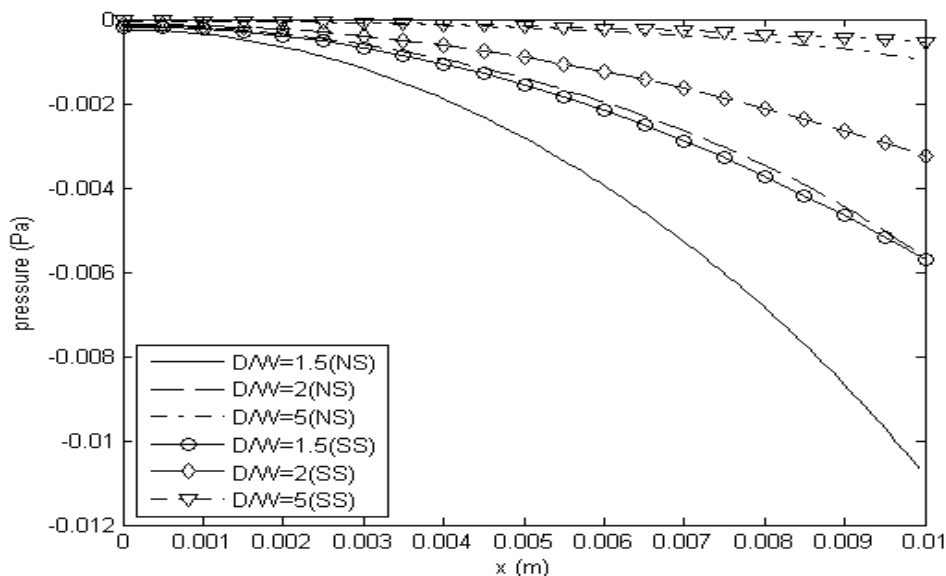


Fig. 5 Pressure variations parallel to the wall within boundary layer thickness at  $y=0.001\text{m}$

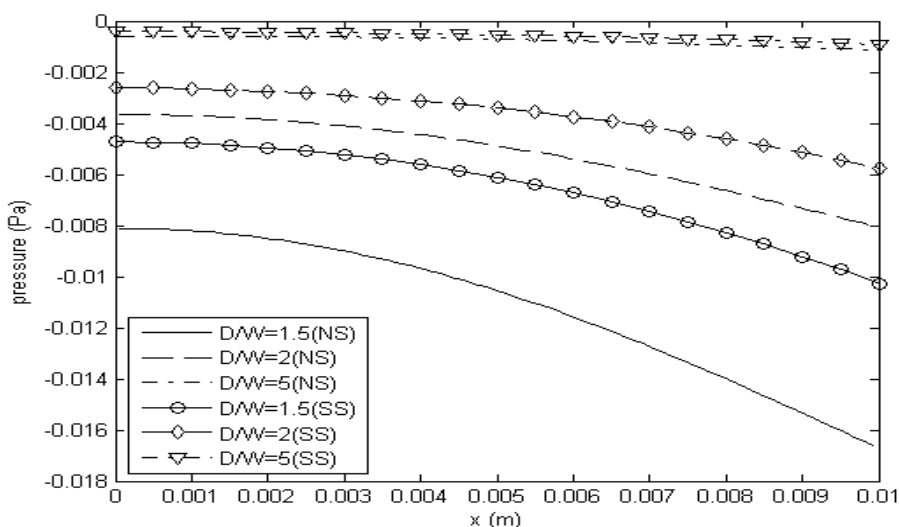


Fig. 6 Pressure variations parallel to the wall outside the boundary layer thickness at  $y=0.01\text{m}$

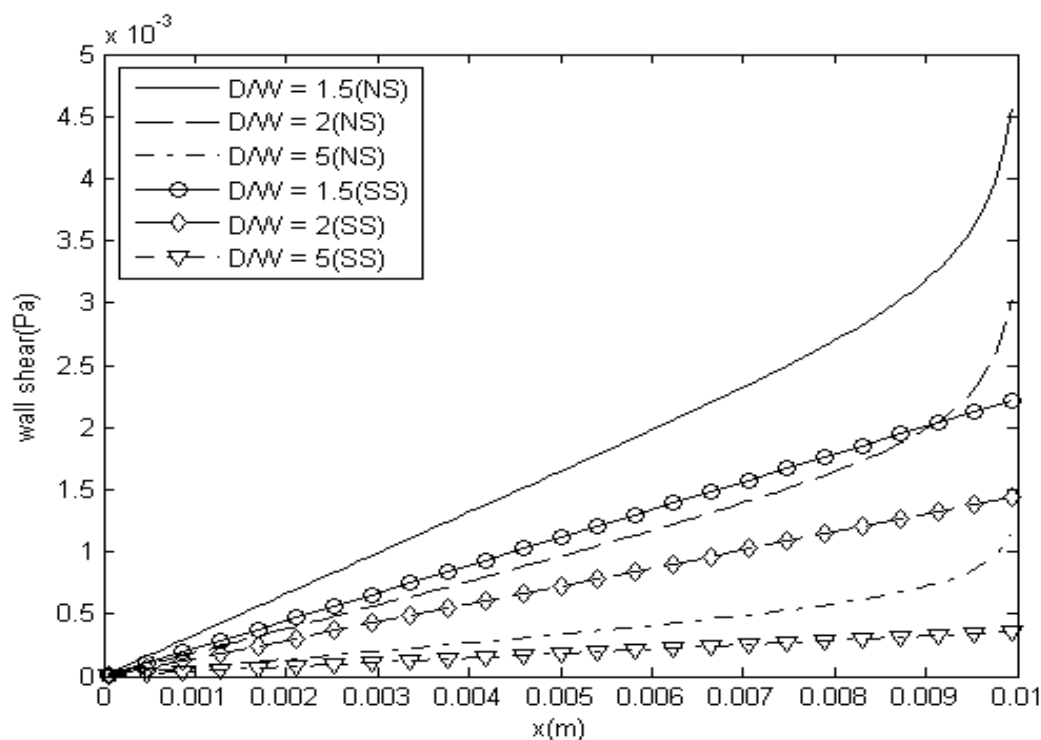


Fig. 7 Distribution of wall shear stress

#### IV. CONCLUSION

This study provides a numerical testing of the distribution of pressure and wall shear stress in stagnation-point flow. Numerical findings show that pressure variation obtained from similarity solution and numerical simulation are in tremendously good agreement for large aspect ratio and in region close to the stagnation point. Discrepancy of results in pressure profiles increases as aspect ratio decreases and in region which is away from the stagnation point. Results from numerical simulation show that pressure variation normal to the wall and within the boundary layer is negligibly small, which is consistent with those predicted by similarity solution. Both similarity solution and numerical simulation give good agreement of pressure distribution parallel to the wall with high aspect ratio in the region which is within or outside the boundary layer. Numerical simulation finds that results of wall shear stress are larger than those predicted by similarity solution. But the variation of wall shear stress with  $x$  has been observed. It is concluded that in order to simulate more accurately the stagnation-point flow, high aspect ratio should be chosen

#### ACKNOWLEDGMENT

V. K. Sin thanks comments from the reviewers and Computational Engineering Laboratory of Department of Electromechanical Engineering, University of Macau for using its facility.

#### REFERENCES

- [1] G. I. Burde, "Non-Steady Stagnation-Point Flows over Permeable Surfaces: Explicit Solution of the Navier-Stokes Equations," *ASME J. of Fluids Engineering*, 117(1) (1995), pp. 189-191.
- [2] K. Hiemenz, Göttingen dissertation; and *Dinglers Polytech. J.*, Vol. 326, p. 311, 1911.
- [3] V. K. Sin, and T. Y. Tong, "Simulation of Stagnation-Point Flow and Analysis of Nonzero Vorticity Region," *Proceedings of the 2008 Asia Simulation conference - 7<sup>th</sup> International conference on System Simulation and Scientific Computing (ICSC'2008)*, October 10-12, 2008, Fragrant Hill Hotel, Beijing, China, pp. 1453-1456. IEEE Catalog Number: CFP0858D-CDR, ISBN: 978-1-4244-1787-2, Library of Congress: 2007907366.
- [4] V. K. Sin, T. Y. Tong, "Comparison of Numerical Simulation of 2-D Stagnation-Point Flow with Similarity Solution," *Proceedings of The International Conference of Numerical Analysis and Applied Mathematics 2008 (ICNAAM 2008)*, The Third Symposium on Numerical Analysis of Fluid Flow and Heat Transfer, September 16-20, 2008, Kos, Greece, pp. 763-766, American Institute of Physics (AIP) Conference Proceedings, ISBN 978-0-7354-0576-9.
- [5] F. M. White, *Viscous Fluid Flow*, McGraw-Hill book Company, New York, 1974.
- [6] L. F. Shampine, I. Gladwell, and S. Thompson, *Solving ODEs with MATLAB*, Cambridge University Press, Cambridge, UK, 2003.
- [7] G. K. Batchelor, *An Introduction to Fluid Dynamics*, Cambridge University Press, Cambridge, UK, 1967
- [8] S. V. Patankar and D. B. Spalding, "A Calculation procedure for heat, mass and momentum transfer in three-dimensional parabolic flows," *Int. J. Heat Mass Transfer*, vol. 15, pp. 1787-1806, 1972.
- [9] R. I. Issa, "Solution of the implicitly discretised fluid flow equations by operator-splitting," *J. Comp. Phys.*, vol. 62, pp.40-65, 1986.
- [10] STAR-CD, Version 3.2, Methodology, Confidential-for authorised users only, CD Adapco Group, 2004.